Influence of water radiolysis on the mobilization of Tc(IV) in bentonite clay

Results from field experiments at Äspö

Mats Jansson, Trygve E Eriksen
Department of Chemistry/Nuclear Chemistry
Royal Institute of Technology

Luis Moreno
Department of Chemical Engineering and
Technology/Chemical Engineering
Royal Institute of Technology

November 2006

SKB

Influence of water radiolysis on the mobilization of Tc(IV) in bentonite clay

Results from field experiments at Äspö

Mats Jansson, Trygve E Eriksen
Department of Chemistry/Nuclear Chemistry
Royal Institute of Technology

Luis Moreno
Department of Chemical Engineering and
Technology/Chemical Engineering
Royal Institute of Technology

November 2006

Preface

A draft of this report was ready during late 2004. The long delay until a final version has been ready is due to a series of reviewer comments, combined with changed priorities within SKB's activities. On the other hand, the content of the report has been greatly improved.

Abstract

Radiolysis will occur when water is exposed to ionizing radiation. Radiolysis of water may locally create oxidizing conditions, which are unfavourable to a repository of KBS-3 type. In this investigation we have studied to what extent water radiolysis products affect the migration (diffusion) in compacted bentonite clay of the redox-sensitive element technetium.

Two cases have been studied, one when an α-radiation source was placed sufficiently far away from the technetium to only have molecular water radiolysis products reaching the technetium ("indirect radiolysis"). In the other case technetium was placed in direct contact with an α-radiation source and hence both radical and molecular water radiolysis products reached the technetium ("direct radiolysis").

The experiments were performed in the CHEMLAB probe, a borehole laboratory designed for in situ investigations. The radiation sources and experiment cells containing compacted bentonite and Tc(IV) were prepared and placed in CHEMLAB in a conventional laboratory before the probe was installed in borehole KJ0052F02 located at 450 m depth at Äspö HRL.

After groundwater saturation of the bentonite in the indirect radiolysis experiment, groundwater was pumped in a loop from the reservoir to the irradiation chamber, past the inlet filter of the experiment cell and back to the reservoir. In this way the concentration of molecular water radiolysis products, which could diffuse into the cell via the inlet filter, increased during the whole indirect radiolysis experiment.

As the groundwater diffused into the cell of the direct radiolysis experiment, the production of water radiolysis products increased until full water saturation was reached after approximately four weeks when the production reached a steady-state. The experiment lasted 100 days. After termination the bentonite in the cells was sliced in thin sections, dried, weighed and analyzed for ^{99}Tc-activity.

In the indirect radiolysis experiment the technetium migrated very slightly if at all. This is probably due to the very slow kinetics of the oxidation of Tc(IV) in the aqueous phase by O_2 and H_2O_2.

In the direct radiolysis experiment technetium had clearly started to migrate from its original position. This indicates that either $OH^\bullet$ and $CO_3^{-\bullet}$ are involved in the oxidation process or that the local concentration of H_2O_2 is sufficiently high to oxidize TcO_2.

Sammanfattning

Joniserande strålnings sönderdelning av vatten kallas vattenradiolys. Vattenradiolys kan lokalt skapa oxiderande förhållanden, vilket är ogynnsamt för ett djupförvar av utbränt kärnbränsle av KBS-3 modell. I denna undersökning har vi studerat i vilken omfattning vattenradiolysprodukter påverkar migrationen (diffusionen) av det redoxkänsliga grundämnet teknetium i kompakterad bentonitlera.

Två olika fall har studerats, ett där en α-strålkälla var placerad tillräckligt långt från det reducerade (fyrvärda) teknetiet för att endast stabila molekylära vattenradiolysprodukter skulle nå fram ("indirekt radiolys"). I det andra fallet placerades teknetium i direkt kontakt med en α-strålkälla så att såväl radikal- som molekylära vattenradiolysprodukter kunde nå teknetiet ("direkt radiolys").

Experimenten genomfördes i CHEMLAB-sonden, ett borrhålslaboratorium som designats speciellt för in situ undersökningar. Strålkällor och experiment celler preparerades och placerades i CHEMLAB på ett vanligt "ovanjordlaboratorium" innan sonden installerades i ett borrhål beläget 450 m under jord i Äspö HRL.

Efter att bentoniten grundvattenmättats i det indirekta radiolysexperimentet pumpades vattnet som kom i kontakt med experimentcellen i en loop från en reservoar till en bestrålningskammare vidare förbi experimentcellen och sedan tillbaks till reservoaren. På detta sätt ökade koncentrationen av molekylära vattenradiolysprodukter, som kunde diffundera in i experimentcellen via filtret, under hela experimentet.

I det direkta radiolysexperimentet statade radiolysen när grundvattnet nådde strålkällan som var placerad i cellens botten. Efter 100 dagar avslutades försöket och bentoniten i experimentcellen skivades i tunna snitt, torkades, vägdes innan ^{99}Tc-aktiviteten mättes med en γ-detektor.

I det direkta radiolysexperimentet hade teknetiet rört sig mycket litet om alls. Detta beror förmodligen på att O_2 och H_2O_2 oxiderar Tc(IV) mycket långsamt i vattenlösning.

I det direkta radiolysexperimentet hade teknetiet helt klart rört sig från sin ursprungsposition. Detta indikerar att antingen är OH$^{\bullet}$ och CO$_3^{-\bullet}$ inblandade i oxidationsprocessen eller så är H_2O_2-koncentrationen tillräckligt hög för att oxidation av TcO_2 ska kunna ske.

Contents

1   Introduction

In a deep repository of KBS-3 type many of the processes that affect the long-time safety – such as dissolution of the uranium dioxide matrix, corrosion of the copper canister and the mobility of redox sensitive elements (Pu, Np, Am, Tc, etc) – rely on stable reducing conditions. When, for instance, technetium is oxidized from its tetravalent state to the heptavalent pertechnetate ion (TcO_4^-), the element will be much more mobile, since the retention (due to sorption on mineral surfaces) of anions is very low. In an earlier through diffusion experiment in CHEMLAB it was demonstrated that pertechnetate diffused unreduced through a 1 cm thick bentonite plug despite reducing conditions /Jansson and Eriksen 2003/. The Tc-profile in the diffusion cell showed a few Tc peaks, which were interpreted as Tc-reduction at iron-containing minerals in the bentonite.

Upon absorption of ionizing radiation by water, oxidizing and reducing radiolysis products are formed, which locally can change the redox conditions. The purpose of the present radiolysis project is to investigate to what extent Tc is mobilized by oxidation of Tc(IV) by radiolysis products formed in natural groundwater on irradiation with a well defined α-radiation source. The influence of molecular products as well as the influence of molecular and radical water radiolysis products are examined.

2   Water radiolysis

When ionizing radiation meets water, it will interact with the water forming excited and ionized water molecules:

$$H_2O \rightarrow H_2O^* \tag{2.1}$$

$$H_2O \rightarrow H_2O^+ + e^- \tag{2.2}$$

The electrons formed upon ionization of water are thermalized and then hydrated:

$$e^- \rightarrow e^-_t \rightarrow e^-_{aq} \tag{2.3}$$

The excited water molecules dissociate homolytically within 10^{-13} s:

$$H_2O^* \rightarrow H^\bullet + OH^\bullet \tag{2.4}$$

Thus, irradiation of water primarily yields e^-_{aq}, $H^\bullet$ and $OH^\bullet$ as highly reactive species. H_2O^+ is a strong acid and will undergo proton transfer reactions with the surrounding water:

$$H_2O^+ + H_2O \rightarrow OH^\bullet + H_3O^+ \tag{2.5}$$

i.e. $OH^\bullet$ radicals, H_3O^+ ions and e^-_{aq} are produced within a very short time span:

$$2\ H_2O \xrightarrow{\text{ionizing radiation}} H_3O^+ + OH^\bullet + e^-_{aq} \tag{2.6}$$
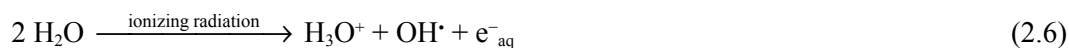
The molecular by-products H_2 and H_2O_2 are formed from the primary radicals:

$$OH^\bullet + OH^\bullet \rightarrow H_2O_2 \tag{2.7}$$

$$H^\bullet + H^\bullet \rightarrow H_2 \tag{2.8}$$

$$e^-_{aq} + H^\bullet\ H_2O \rightarrow H_2 + OH^- \tag{2.9}$$

$$e^-_{aq} + e^-_{aq} + 2\ H_2O \rightarrow H_2 + 2\ OH^- \tag{2.10}$$

Molecular oxygen is formed from H_2O_2 through slower reactions.

The primary radicals can also combine to re-form water:

$$H^\bullet + OH^\bullet \rightarrow H_2O \tag{2.11}$$

$$e^-_{aq} + OH^\bullet \rightarrow OH^- \tag{2.12}$$

$$H_3O^+ + OH^- \rightarrow H_2O \tag{2.13}$$
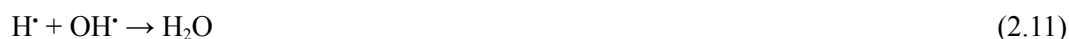
The above reactions are examples of how molecular products are formed. Apart from those, a number of radical reactions take place where some other species are formed as well.

Since the *LET*-value (Linear Energy Transfer, the energy absorbed per unit path length of absorber) is much higher for alpha radiation, than for beta and gamma radiation, the alpha dose rate will locally be much higher than that of beta and gamma. Alpha radiation will thereby locally produce oxidants in higher concentrations than beta and gamma radiation, see also G-values in Table 2-1 (the G-value is the radiation chemical yield in molecules per unit absorbed energy). In a mixed radiation field the hydrogen atoms, hydroxyl radicals and electrons formed on water radiolysis by beta and gamma radiation will consume some of the molecular oxidants (H_2O_2 and O_2) produced from alpha radiation.

Thus, water radiolysis will produce molecular stable species, O_2, H_2O_2 and H_2, and a number of highly reactive radicals. Many of these species may oxidize radionuclides in a nuclear waste repository to a state where they are more mobile than in reduced form.

Table 2-1. G-values in neutral water for radiolysis of water [molecules/100 eV].

	H_2O	H_2	H_2O_2	e^-_{aq}	$H^{\cdot}$	$OH^{\cdot}$	H^+	$HO_2^{\cdot}$
$G(\alpha)^a$	−2.71	1.3	0.985	0.06	0.21	0.24	0.06	0.22
$G(\beta,\gamma)^b$	−4.15	0.475	0.75	2.8	0.6	2.8	2.8	0

[a]/Eriksen et al. 1987/, [b]/Choppin et al. 1996/

3 Experimental

3.1 Materials

3.1.1 Technetium

Technetium was selected as the element to be studied since:

- The oxidation of Tc(IV) to Tc(VII) is a three-electron process. This makes Tc(IV) relatively hard to oxidize (the reaction rate is slow), but once oxidized, the reduction of Tc(VII) is kinetically relatively slow as well, see further Figure 3-1.

- Pertechnetate is an anion and will sorb but slightly to the negatively charged mineral surfaces of the bentonite, i.e. the retardation of pertechnetate will be distinctly lower than that of a cation, making the diffusion faster and hence the influence of radiolysis products on the mobilization easier to detect.

The pertechnetate solution was prepared from analytical grade chemicals by adding small aliquots of the stock solution to the solution used in the experiment. The radionuclide used, ^{99}Tc (Amersham), was obtained in aqueous acid solution.

Reduced technetium was obtained by irradiating a pertechnetate solution in a gamma source for 12 hours. A black precipitation of amorphous $TcO_2 \cdot n\,H_2O$ (as well as black colloidal particles) was formed. The precipitate was then filtered from the solution.

3.1.2 Bentonite

The bentonite used in this investigation was the American Colloid Co, type MX-80 (Wyoming Na-bentonite). The bentonite (MX-80) has a clay content (< 2 µm) of approximately 85% and a montmorillonite $(Na_{0.36}Ca_{0.2}[Si_{7.96}Al_{0.04}](Al_{3.1}Mg_{0.56}Fe^{II}_{0.16}Fe^{III}_{0.18})O_{20}(OH)_4$ /Marry et al. 2002/) content of 80–90 wt% of this fraction. The remaining silt fraction contains quartz, feldspar and some micas, sulphides and oxides /Pusch and Karnland 1986/, see Table 3-1 for more specific data on the bentonite.

In the experiments the bentonite was compacted to a dry density of 1.8 g $\cdot$ cm^{-3}. At that compaction the total porosity is 0.32. The bentonite was assumed to be fully water saturated, i.e. the water content was assumed to be 15% (weight).
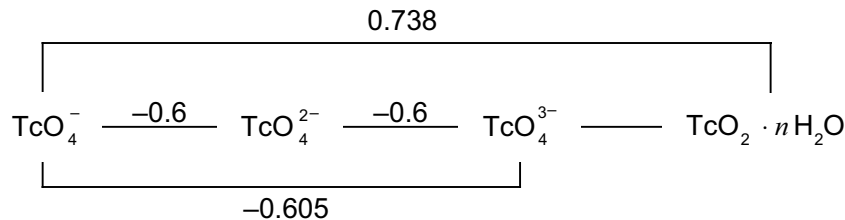
**Figure 3-1.** *Reduction potentials for the Tc(IV)-Tc(VII) system. /Eriksen et al. 1992/.*

Table 3-1. Bentonite data

Parameter	MX-80
Cation-exchange capacity, $[X]_T$	0.75 meq g^{-1}
Amphoteric edge sites, $[SOH]_T$	28.4 µmol g^{-1}
Edge surface area	3.0 m2 g^{-1}
Exchangeable Na	80.8%
Exchangeable Ca	12.8%
Exchangeable Mg	5.5%
Exchangeable K	0.9%
Total carbonate (as $CaCO_3$)	1.5 wt%
Total quartz	~23 wt%
$CaSO_4$ impurity	0.58 wt%
$MgSO_4$ impurity	0.02 wt%
NaCl impurity	0.01 wt%
KCl impurity	0.01 wt%
Specific density	2,700 kg m^{-3}

3.2   The CHEMLAB-1 probe

The radiolysis experiments were performed in the CHEMLAB-1 probe (see Figure 3-2), which is a borehole laboratory equipped with two pumps, six multi-channel valves, solution reservoirs and a fraction collector /Jansson and Eriksen 1998, 2001/. The radiolysis experiments were performed in borehole KJ0052F02 located at 450 m depth at Äspö HRL. Preparation of the experiment cells and the radiation sources were performed at an above ground laboratory. After the laboratory preparations the CHEMLAB probe was transported to the experiment site in the Äspö tunnel (borehole KJ0052F02) where the whole probe system (packer and the six CHEMLAB sections) was assembled and pushed into the borehole. The system was then pushed 18 metres to full depth of the borehole where a water carrying fracture is situated. The packer was expanded to seal off the test section in the borehole and all flow paths were flushed with groundwater before the experiment was started.

The composition of the groundwater is given in Table 3-2.
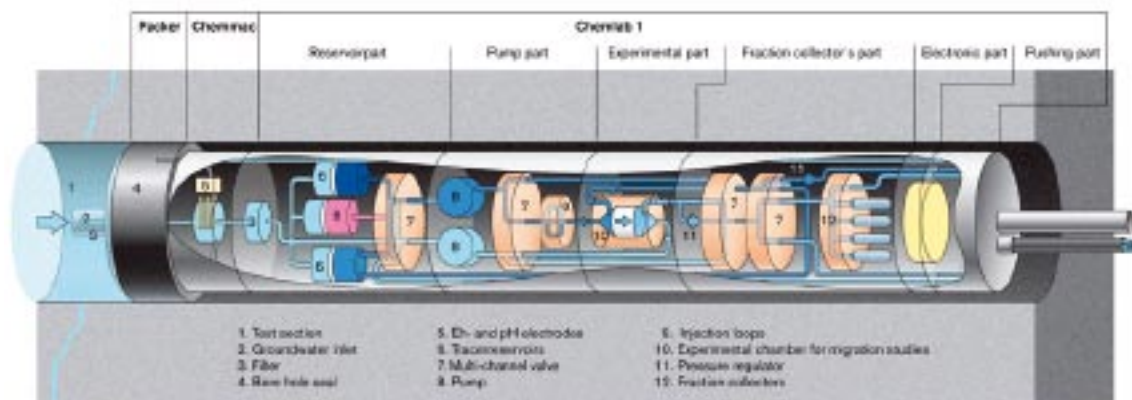
Figure 3-2. *Principal drawing of the CHEMLAB-1 probe.*

Table 3-2. Groundwater composition for borehole KJ0052F02, sampled 2002-09-18 /Carmström 2003/.

| Element	Concentration [mg/L]	Element	Concentration [mg/L]
Na	2,370	F	2.04
K	8.81	Si	5.6
Ca	2,360	Fe, tot	0.121
Mg	47	Fe^{2+}	0.095
HCO_3^-	22	Mn	0.37
Cl	7,979.3	Li	1.67
SO_4	492.2	Sr	41.3
SO_4_S*	155	DOC	1.2
Br	51.78		
El. conductivity	2,192 mS/m	pH	7.4

*SO_4_S = sulphate analysed as sulphur

3.3   Experiment concept

Two different cases were studied simultaneously in CHEMLAB-1. In one case the influence of molecular water radiolysis products on the mobility of Tc(IV) in compacted bentonite clay was studied ("indirect radiolysis"), while in the other case the influence of primary as well as secondary formed water radiolysis products was studied ("direct radiolysis").

3.3.1   Indirect radiolysis

In the indirect radiolysis the diffusion cell, a cylinder with a diameter of 10 mm and length 10 mm (volume = 0.785 cm³), was sealed at one end. The cell was filled halfway with bentonite compacted to a dry density of 1.8 g cm⁻³. A few (4–5) grains tetravalent technetium as $TcO_2 \cdot n\,H_2O(s)$, corresponding to approximately 50 kBq ^{99}Tc (corresponding to about 0.8 μmol) were placed on top of the compacted bentonite before the rest of the cell was filled with bentonite and subsequently compacted to a dry density of 1.8 g cm⁻³. The cell was then equipped with a filter, see further Figure 3-3. Ten small ^{241}Am sources (from smoke detectors) were used in the experiments as α-radiation source, see Section "Radiation sources" below.

The cell was first saturated and equilibrated with groundwater by pumping groundwater past the inlet filter for four weeks. After saturation the water passing the inlet filter was circulated in a loop containing a reservoir, pump and α-radiation source. Hence the concentration of molecular water radiolysis products in the circulating water continuously increased with time. Since the irradiation cell was placed some 10 cm before the cell and the flow rate was low, all radicals produced had reacted before reaching the filter of the cell. The remaining water radiolysis products (H_2O_2, O_2 and H_2) could diffuse into the cell and eventually reach the technetium.
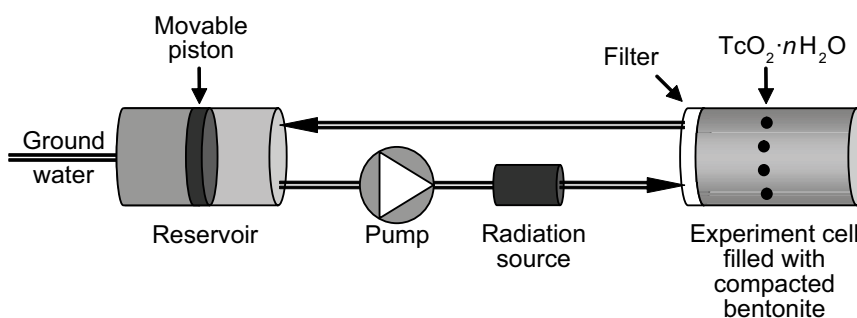
Figure 3-3. Experimental set-up for the indirect radiolysis experiment.

The reservoir is equipped with a moveable piston. The chamber at one side of the piston is connected to the groundwater while the solution used in the experiment is at the other side. When the volume at the experiment side is changed, the piston will follow and make up for the change in pressure. Hence the pressure in the experiment will remain the same as the pressure of the groundwater during the experiment.
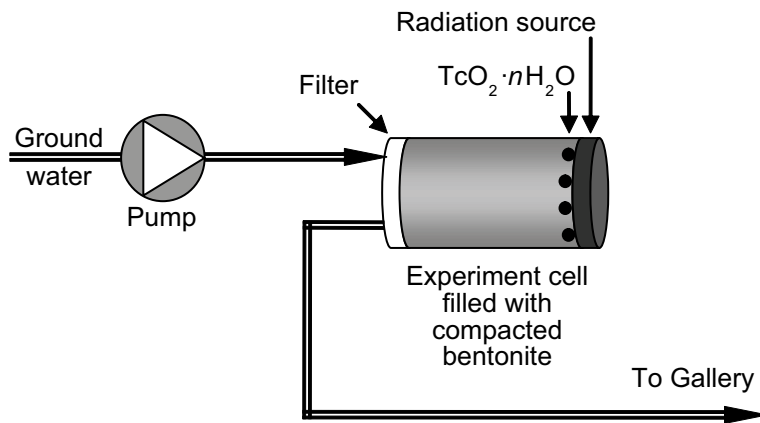
3.3.2 Direct radiolysis

In the experiment where the influence of molecular and radical water radiolysis products was studied (direct radiolysis) a ^{241}Am radiation source was used. The radiation source was placed at the bottom of a diffusion cell which had a diameter of 25 mm and a length of 20 mm (i.e. the volume of compacted bentonite in this experiment was 9.82 cm^3). A few (again 4–5) grains technetium powder were placed directly on the irradiation source before the cell was filled with bentonite compacted to a dry density of 1.8 g cm^{-3}, see Figure 3-4.

Groundwater was then pumped past the inlet filter, allowing the groundwater to saturate the bentonite. When water reached the radiation source at the bottom of the cell, water radiolysis started. Water radiolysis of course started to some extent earlier, since dry bentonite contains 10% water. The water content gradually increased (as did the extent of radiolysis) during the saturation process. Altogether, the water saturation and radiolysis step lasted for 120 days.

3.4 Analysis

The ^{99}Tc activity profiles were obtained by slicing the bentonite plugs from the experiment cells into thin sections. All solid samples were dried, weighed and analyzed for activity using a liquid scintillation detector.

Figure 3-4. *Experimental set-up for the direct radiolysis experiment.*

3.5   Radiation sources

The radiation sources used were in both experiments ^{241}Am with the decay characteristics $t_{1/2}$ 458 y, E_α 5.485 (86%) and 5.443 (14%) MeV.

In the indirect radiolysis experiment groundwater was irradiated using ten small ^{241}Am sources for smoke detectors with total nominal activity 7.4 MBq. Taking the range of the α-radiation in ground water to be 37 μm and the active surface area 1.1 cm^3 we obtain an average dose rate of 0.73 Gy in 4.07 · 10^{-3} cm^{-3} irradiated solution.

The diameter of the active surface of the source used for direct radiolysis experiment was 25 mm and the nominal activity 35.7 MBq. The ^{241}Am source was incorporated in a gold matrix on silver backing and the α-emitting surface covered by a 2 μm thick gold-palladium alloy. The average energy of the degraded α-spectrum as determined by α-spectroscopy using a surface barrier detector was 4.6 MeV. The dose rate in water was determined to be 0.73 Gy s^{-1} /Eriksen et al. 1988/.

Calculation of the radiation dose distribution in water saturated compacted bentonite in contact with the radiation emitting surface requires detailed knowledge of the bentonite particle-water distribution at the bentonite-radiation source interface. Not knowing this we choose to rely on earlier experimental observations. Measuring the yield of H$_2$ in water saturated compacted bentonite with dry density 1.8 g cm^{-3}, using the ^{241}Am radiation source used in the present experiments; the experimental data could best be accommodated by assuming a 20 μm water layer at the interface. The volume of the irradiated water volume is, based on this assumption 1.02 · 10^{-2} cm^{-3} /Eriksen et al. 1987/.

The rate of production of primary radiolysis products, calculated using the G-values given in Table 2-1 and the dose rate of the radiation source used in the direct radiolysis experiment are given in Table 3-3.

The G-values for H$_2$, H$_2$O$_2$ and O$_2$ in carbonate containing solutions and synthetic groundwater have in earlier experiments with the larger ^{241}Am radiation source been determined to be 1.03, 0.69 and 0.15 molecules/100 eV, respectively.

Table 3-3. Rate of production of primary radiolysis products in the compacted bentonite.

Species	Rate of production [μmol dm^{-3} s^{-1}]	[mol s^{-1}]
H$_2$	0.095	1.0 · 10^{-12}
H$_2$O$_2$	0.075	8.1 · 10^{-13}
e$^-_{aq}$	0.005	5.4 · 10^{-14}
H$^\bullet$	0.016	1.7 · 10^{-13}
OH$^\bullet$	0.018	1.9 · 10^{-13}
HO$_2^\bullet$	0.017	1.8 · 10^{-13}
H$^+$	0.005	5.4 · 10^{-14}

Table 3-4. Calculated rates of production of molecular radiolysis products in the irradiated groundwater, based on the G-values given in Table 3-3 and dose rate of the α-source used in the indirect radiolysis experiment.

| Species	Rate of production [mol s^{-1}]	Amount produced in 100 days [mol]	Concentration increase in loop solution [mol dm^{-3} s^{-1}]
H$_2$	3.1 · 10^{-13}	2.7 · 10^{-6}	6.2 · 10^{-12}
H$_2$O$_2$	2.1 · 10^{-13}	1.8 · 10^{-6}	4.2 · 10^{-12}
O$_2$	0.45 · 10^{-13}	0.39 · 10^{-6}	0.9 · 10^{-12}

4   Results and discussion

4.1   Indirect radiolysis

The results from the indirect radiolysis experiment where the water radiolysis products were allowed to diffuse into the cell are displayed in Figure 4-1. As can be seen, the activity distribution indicates that the technetium has migrated very slightly – if at all – from its initial position at $x = 0.5$ cm.
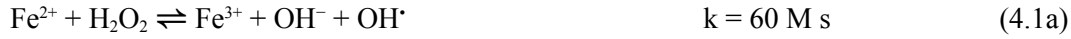
A cell identical to the one used in the experiment, with reduced technetium in compacted bentonite, was produced in order to examine the activity distribution in a system solely saturated with reducing water. The cell was saturated with water, equilibrated with 2 bars H_2. After two weeks saturation the cell was sliced, dried, weighed and analyzed for activity, revealing that the activity distribution was similar to that in the CHEMLAB experiment, see Figure 4-1. The activity distribution in the CHEMLAB experiment most probably is a measure of how well the cell was prepared.

The H_2O_2 and O_2 generated in the indirect radiolysis experiment is diluted into 50 cm^3 groundwater circulating past the cell filter and 0.25 cm^3 bentonite pore water. The initial concentrations of HCO_3^- and Fe^{2+} in the groundwater were 0.36 mM and 1.7 µM, respectively. In an experimental radiation and Mössbauer study of MX-80 bentonite, /Eriksen and Jacobsson 1983/ determined the Fe(II) content of the clay accessible to scavenging of oxidative radicals to be at least 0.4 % and the concentrations of HCO_3^- and Fe^{2+} in the bentonite pore water to be 65 and 0.22 µM, respectively. The Fe^{2+} concentration is probably solubility limited. The total H_2O_2 and O_2 generated in 100 days are 1.8 and 0.39 µmol, respectively (Table 3-4), and the Fe^{2+} in the circulating groundwater will consume $4.3 \cdot 10^{-8}$ mol H_2O_2. If stable in the bentonite environment, the highest possible concentrations of H_2O_2 and O_2 in bentonite pore water of the indirect experiment would be 36 and 7.8 µM, respectively.
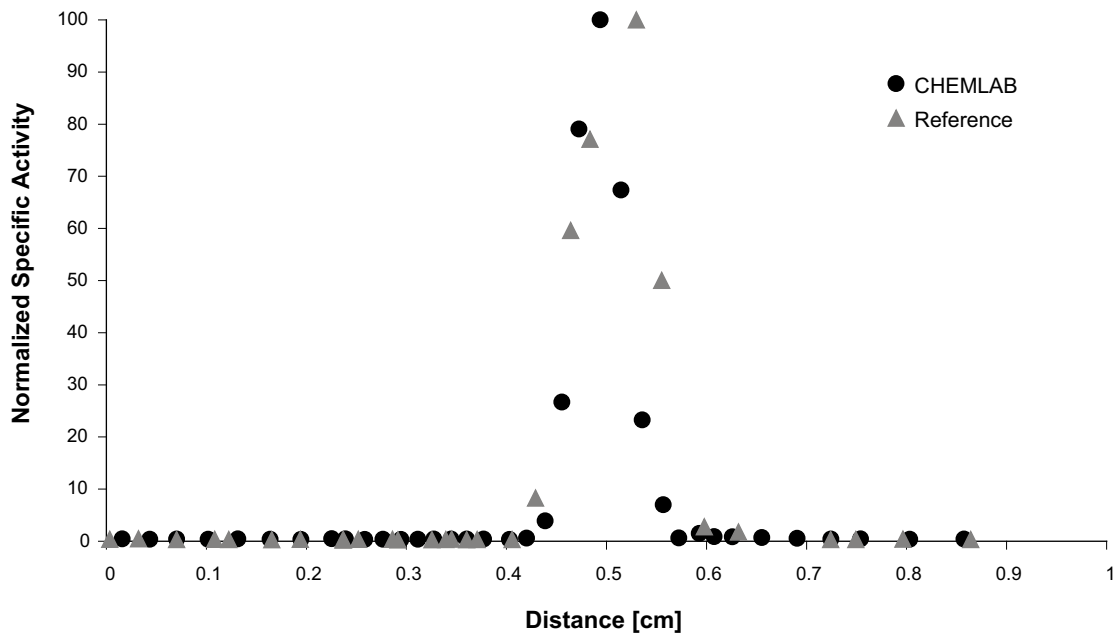
Figure 4-1. *Activity profile in the bentonite cell obtained in the indirect radiolysis. Distance = 0 at the bottom of the cell. The grey triangles were obtained in the reference cell.*
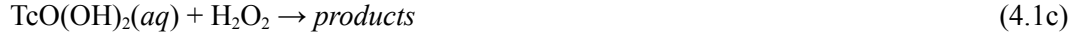
If the dissolution of Fe^{2+} into the pore water is sufficiently fast to maintain the concentration constant, the competing reactions would be

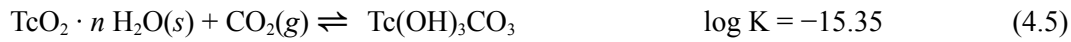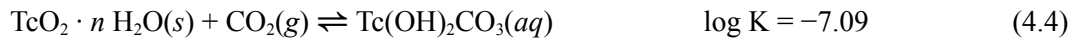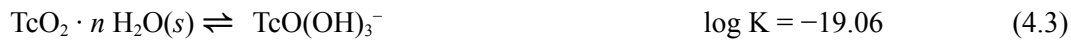$$Fe^{2+} + H_2O_2 \rightleftharpoons Fe^{3+} + OH^- + OH^{\bullet} \qquad\qquad k = 60\ M\ s \qquad (4.1a)$$

which is followed by

$$Fe^{2+} + OH^{\bullet} \rightarrow Fe^{3+} + OH^- \qquad\qquad (4.1b)$$

(i.e. two Fe^{2+} are consumed by one H_2O_2)

$$TcO(OH)_2(aq) + H_2O_2 \rightarrow products \qquad\qquad (4.1c)$$

The expected oxidation product of Tc(IV) is TcO_4^-. The solubility of $TcO_2 \cdot n\ H_2O(s)$ in carbonate containing reducing groundwater is given by the following speciation and equilibrium constants /Eriksen et al. 1992/:

$$TcO_2 \cdot n\ H_2O(s) \rightleftharpoons TcO(OH)_2(aq) \qquad\qquad \log K = -8.17 \qquad (4.2)$$

$$TcO_2 \cdot n\ H_2O(s) \rightleftharpoons TcO(OH)_3^- \qquad\qquad \log K = -19.06 \qquad (4.3)$$

$$TcO_2 \cdot n\ H_2O(s) + CO_2(g) \rightleftharpoons Tc(OH)_2CO_3(aq) \qquad \log K = -7.09 \qquad (4.4)$$

$$TcO_2 \cdot n\ H_2O(s) + CO_2(g) \rightleftharpoons Tc(OH)_3CO_3 \qquad \log K = -15.35 \qquad (4.5)$$

The concentration of Tc(IV) is thus expected to be limited by solubility constrains to $< 10^{-8}\ M$ and $TcO(OH)_2(aq)$ the dominant species.

The detection limit for mobilization of the deposited activity is estimated to be 1% of the total activity, i.e. $0.8\ \mu mol \cdot 0.01 = 8 \cdot 10^{-9}$ mol. The rate constant for equation 4.1c can then be estimated from the following expression:

$$\frac{dc}{dt} = k[TcO(OH)_2][H_2O_2] \qquad\qquad (4.6a)$$

or

$$k = \frac{c_{Tc(VII)}}{[TcO(OH)_2][H_2O_2] \cdot t} \qquad\qquad (4.6b)$$

where $c_{Tc(VII)} = 8 \cdot 10^{-9}$ mol/0.25 mL, $[TcO(OH)_2] = 6.8 \cdot 10^{-9}\ M$, $[H_2O_2] = 36 \cdot 10^{-6}\ M$ and $t = 100$ days. The rate constant for reaction (4.1c) is thus $< 15\ M^{-1}\ s^{-1}$

In a series of experiments Eriksen and Cui /Eriksen and Cui 1991/ observed no desorption of $TcO(OH)_2(s)$ sorbed on granite into aerated synthetic groundwater. On addition of a high concentration ($0.6–1.4\ mol\ dm^{-3}$) of H_2O_2 substantial desorption occurred within 1–2 days. These data indicate the rate of oxidization of Tc(IV) by O_2 and even by H_2O_2 to be very low.

It ought to be emphasized that decomposition of H_2O_2 to O_2 and H_2O_2 consumption by Fe^{2+} during diffusion into the position of the deposited Tc(IV) also may be a reason for the absence of Tc-mobilization in the indirect experiment.

4.2 Direct radiolysis

The activity distribution from the direct radiolysis experiment where compacted bentonite with deposited technetium was placed in direct contact with the radiation source is displayed in Figure 4-2.

The points up to 2 mm are probably reduced Tc, the variation in specific activity is due to that the Tc was added as grains. The points above 2 mm clearly show that the Tc has moved.

In earlier CHEMLAB studies it was observed that once oxidized to its heptavalent state, Tc diffused unreduced through a 1 cm thick bentonite plug despite reducing conditions /Jansson and Eriksen 2004/. Assuming that heptavalent Tc will not be reduced and that a constant flux of technetium is entering the cell (i.e. constant dissolution rate of Tc(IV)), the system can be modelled according to:

The activity balance for Tc in the bentonite may be written as

$$\varepsilon_p \frac{\partial C}{\partial t} = D_{eff} \frac{\partial^2 C}{\partial x^2}$$

(4.7)

where ε_p is the porosity of the bentonite and D_{eff} the effective diffusivity (m²/s). C is the activity in the pore water (cps/m³ water), t time (s) and x distance (m). The equation may be expressed in function of the apparent diffusivity

$$\frac{\partial C}{\partial t} = D_a \frac{\partial^2 C}{\partial x^2}$$

(4.8)

The solution from literature is /Carslaw and Jaeger 1959/

$$C = \frac{2 \cdot F_o}{D_{eff}} \left\{ \left(\frac{D_a \cdot t}{\pi} \right)^{0.5} \mathrm{Exp}\left[-\frac{x^2}{4 D_a \cdot t} \right] - \frac{x}{2} \mathrm{Erfc}\left[\frac{x}{2\sqrt{D_a \cdot t}} \right] \right\}$$

(4.9)

The flux, F_0, is expressed taking into account the totality of the cross section area.

From Figure 4-2 it is concluded that Tc(IV) is located between 0–2 mm. Setting 1 mm from the bottom of the cell as origin (from where the Tc flux originates) is then a fair assumption.

The results can then be fitted (Figure 4-3) using an apparent diffusivity of $5 \cdot 10^{-13}$ m² s⁻¹ and a flux (Tc(IV) dissolution rate) of 3.54 cps m⁻² s⁻¹, which corresponds to about $8 \cdot 10^{-11}$ mol m⁻² s⁻¹. The cross section area of the cell is $4.9 \cdot 10^{-4}$ m². The total Tc flux (total oxidized Tc(IV)) would then in 100 days be about $3.4 \cdot 10^{-11}$ mol.

The amount of oxidized technetium in the experiments may be used to derive tentative values for the kinetics of the oxidizing reactions. The major differences between the two experiments are in the supply of oxidants.
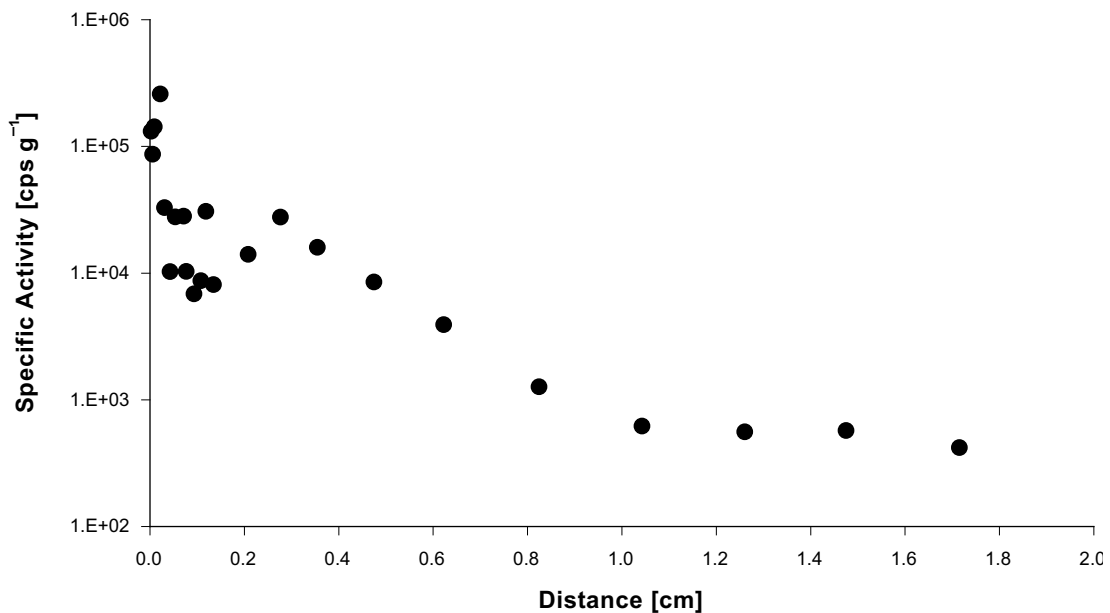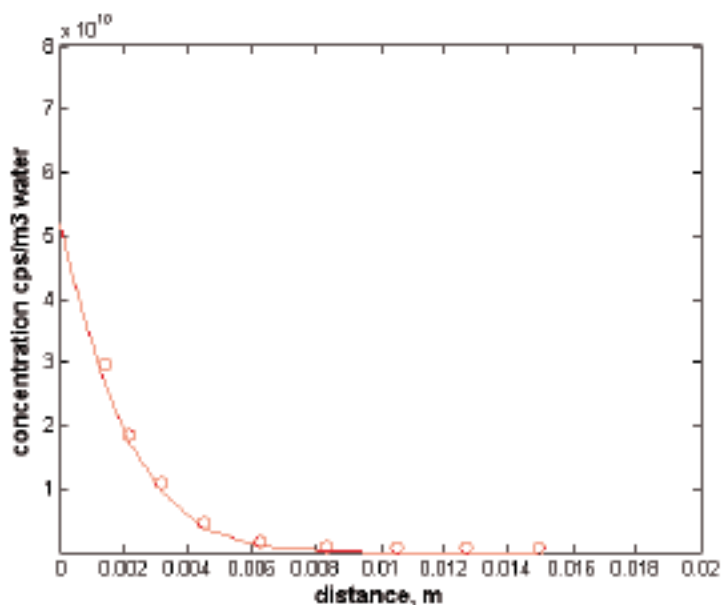

Figure 4-2. *Activity profile in the bentonite cell obtained in the direct radiolysis experiment.*

Figure 4-3. Fitting of the activity profile in the bentonite cell obtained in the direct radiolysis experiment.

For the direct radiolysis experiment, the primary oxidants formed on radiolysis of the pore water are $OH^\bullet$, $HO_2^\bullet$ and H_2O_2. The $OH^\bullet$ radicals, however, react in part with dissolved carbonate ions forming $CO_3^{-\bullet}$. All are potent oxidants with the one-electron reduction potentials given in Table 4-1.

The radiolytic oxidation process in the bentonite pore water is very complex involving radiolysis, dissolution of Fe^{2+} and $Tc(IV)$, redox reactions and diffusion of reactants and products. The reaction scheme is given in Table 4-2.

Based on the discussion above on rate constant limitations for the oxidation of $Tc(IV)(aq)$ by H_2O_2 in the indirect experiment, some calculations have tentatively been carried out using the rate constant 10 M^{-1} s^{-1} for reaction (4.1c), using the kinetic computer code MAKSIMA-CHEMIST /Carver et al. 1979/ and the dose rate for the α-source used in the experiment. The volume considered is $1.02 \cdot 10^{-2}$ cm^{-3}, based on the assumption mentioned in "Radiation Sources". The results of the simulations are plotted as calculated concentrations versus time in Figure 4-4. As can be seen, the production rate for oxidized Tc is at the beginning in the order of 10^{-15} $mol \cdot L^{-1} \cdot s^{-1}$ (at longer times products diffuse out of the system considered). According to the diffusion model discussed above, and illustrated in Figure 4-3, the rate of oxidation of Tc was $3.4 \cdot 10^{-11}$ mol / 100 days = $3.9 \cdot 10^{-18}$ mol s^{-1}, and given the production volume of $1.02 \cdot 10^{-2}$ mL (see "Radiation Sources"), the rate deduced from the experiments becomes $3.9 \cdot 10^{-13}$ $mol \cdot L^{-1} \cdot s^{-1}$. It is therefore apparent that the calculated rate of Tc oxidation using the kinetic model described above is about three orders of magnitude less than observed in the experiment.

Table 4-1. One electron reduction potentials for oxidants formed on radiolysis of pore water /Ekeroth and Jonsson 2003/.

Oxidant	E^0 (V)
$OH^\bullet$	1.90
$CO_3^{-\bullet}$	1.59
$HO_2^\bullet$	0.79
H_2O_2	0.46
O_2	−0.10

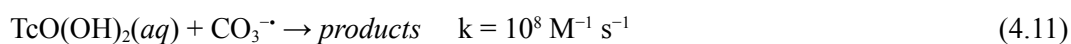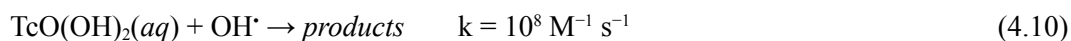**Table 4-2. Radiolytic generated reactions in iron and carbonate containing groundwater.**

Reaction	Reaction Rate
$OH^• + OH^• \rightarrow H_2O_2$	$k = 4.0 \cdot 10^9 \ M^{-1} \ s^{-1}$
$OH^• + e_{aq}^- \rightarrow OH^-$	$k = 2.0 \cdot 10^{10}$
$OH^• + H^• \rightarrow H_2O$	$k = 2.5 \cdot 10^{10} \ M^{-1} \ s^{-1}$
$OH^• + O_2^{-•} \rightarrow OH^- + O_2$	$k = 1.0 \cdot 10^{10}$
$OH^• + H_2O_2 \rightarrow H_2O + O_2^{-•} + H^+$	$k = 2.25 \cdot 10^7 \ M \ s$
$OH^• + H_2 \rightarrow H_2O + H^•$	$k = 4.0 \cdot 10^7$
$e_{aq}^- + e_{aq}^- + 2 \ H_2O \rightarrow OH^- + OH^- + 2 \ H^+$	$k = 5.0 \cdot 10^9 \ M \ s$
$e_{aq}^- + H^• + H_2O \rightarrow OH^- + H_2$	$k = 2.0 \cdot 10^{10}$
$e_{aq}^- + HO_2^• \rightarrow HO_2^-$	$k = 2.0 \cdot 10^{10}$
$e_{aq}^- + O_2^{-•} + H_2O \rightarrow HO_2^- + OH^-$	$k = 1.2 \cdot 10^{10}$
$e_{aq}^- + H_2O_2 \rightarrow OH^• + OH^-$	$k = 1.6 \cdot 10^{10} \ M \ s$
$e_{aq}^- + H^+ \rightarrow H^•$	$k = 2.2 \cdot 10^{10}$
$e_{aq}^- + O_2 \rightarrow O_2^{-•}$	$k = 2.0 \cdot 10^{10}$
$e_{aq}^- + H_2O \rightarrow H^• + OH^-$	$k = 2.0 \cdot 10^1$
$H^• + H^• \rightarrow H_2$	$k = 1.0 \cdot 10^{10} \ M^{-1} \ s^{-1}$
$H^• + HO_2^• \rightarrow H_2O_2$	$k = 2.0 \cdot 10^{10} \ M^{-1} \ s^{-1}$
$H^• + O_2^{-•} \rightarrow HO_2^-$	$k = 2.0 \cdot 10^{10} \ M^{-1} \ s^{-1}$
$H^• + H_2O_2 \rightarrow H_2O + OH^•$	$k = 6.0 \cdot 10^7$
$H^• + OH^- \rightarrow e_{aq}^- + H_2O$	$k = 2.0 \cdot 10^7 \ M^{-1} \ s^{-1}$
$H^• + O_2 \rightarrow O_2^{-•} + H^+$	$k = 2.0 \cdot 10^{10}$
$HO_2^• \rightarrow O_2^{-•} + H^+$	$k = 8.0 \cdot 10^5 \ M \ s$
$HO_2^• + HO_2^• \rightarrow O_2 + H_2O_2$	$k = 7.5 \cdot 10^5$
$HO_2^• + O_2^{-•} \rightarrow O_2 + HO_2^-$	$k = 8.5 \cdot 10^7$
$O_2^{-•} + H^+ \rightarrow HO_2^•$	$k = 5.0 \cdot 10^{10} \ M \ s$
$H_2O_2 + OH^- \rightarrow HO_2^- + H_2O$	$k = 5.0 \cdot 10^8$
$HO_2^- + H_2O \rightarrow H_2O_2 + OH^-$	$k = 5.735 \cdot 10^4$
$H_2O \rightarrow H^+ + OH^-$	$k = 2.599 \cdot 10^{-5} \ M \ s$
$H^+ + OH^- \rightarrow H_2O$	$k = 1.43 \cdot 10^{11} \ M^{-1} \ s^{-1}$
$H^• + H_2O \rightarrow H_2 + OH^•$	$k = 1.1 \cdot 10^{-3}$
$OH^• + CO_3^{2-} \rightarrow CO_3^{-•} + OH^-$	$k = 4.0 \cdot 10^8$
$OH^• + HCO_3^- \rightarrow CO_3^{-•} + H_2O$	$k = 1.5 \cdot 10^6$
$O_2^{-•} + CO_3^{2-} \rightarrow CO_3^{2-} + O_2$	$k = 3.0 \cdot 10^8$
$CO_3^{-•} + CO_3^{-•} \rightarrow CO_4^{2-} + CO_2$	$k = 7.0 \cdot 10^6$
$H_2O_2 + CO_3^{-•} \rightarrow CO_3^{2-} + O_2^{-•} + 2 \ H^+$	$k = 4.3 \cdot 10^5 \ M^2 \ s^2$
$HO_2^{-•} + CO_3^{-•} \rightarrow CO_3^{2-} + O_2^{-•} + H^+$	$k = 3.0 \cdot 10^7 \ M \ s$
$H^+ + HCO_3^- \rightarrow CO_2 + H_2O$	$k = 1.0 \cdot 10^{10}$
$OH^- + HCO_3^- \rightarrow CO_3^{2-} + H_2O$	$k = 1.0 \cdot 10^9$
$H_2O + CO_2 \rightarrow HCO_3^- + H^+$	$k = 8.41 \cdot 10^1$
$H_2O + CO_3^{2-} \rightarrow HCO_3^- + OH^-$	$k = 3.8 \cdot 10^3$
$H_2O + CO_4^{2-} \rightarrow CO_3^{2-} + H_2O_2$	$k = 2.0 \cdot 10^{-1}$
$Fe^{2+} + OH^• \rightarrow Fe^{3+} + OH^-$	$k = 3.4 \cdot 10^8$
$Fe^{2+} + CO_3^{-•} \rightarrow Fe^{3+} + CO_3^{2-}$	$k = 1.0 \cdot 10^8$
$Fe^{2+} + H_2O_2 \rightarrow Fe^{3+} + OH^• + OH^-$	$k = 6.0 \cdot 10^1 \ M \ s$
$Fe^{2+} + HO_2^• \rightarrow Fe^{3+} + HO_2^-$	$k = 1.2 \cdot 10^6 \ M \ s$
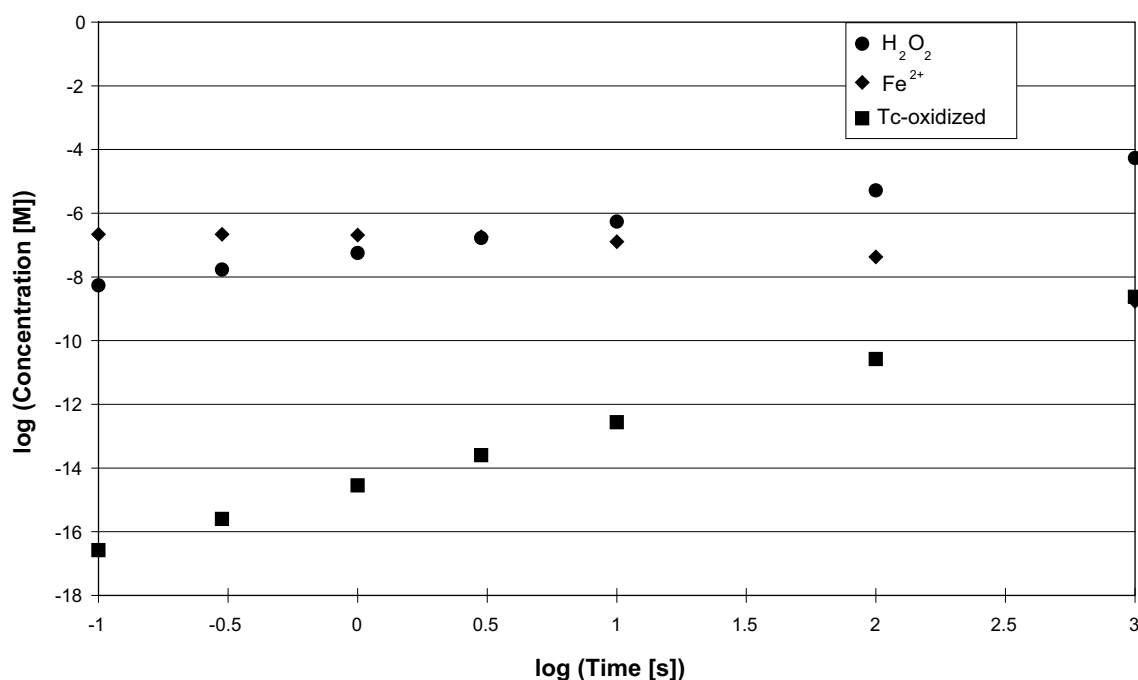
Figure 4-4. *Concentration of H_2O_2, Fe^{2+} and oxidized technetium obtained in simulations based on the dose rate of the α-radiation source used in the experiments and the reactions given in Table 4-2 and a rate constant of 10 M^{-1} s^{-1} for reaction 4-1c. Initial concentrations of Tc(IV), HCO_3^- and Fe^{2+} were set to be 10^{-8} M, 0.36 mM and 1.7 μM, respectively.*

Additional computer simulations have also been performed in order to try to obtain a better agreement between the observed and calculated oxidation rates of Tc. Calculation results showing the effect of varying the rate constant for oxidation of Tc(IV) by H_2O_2 (reaction 4.1c) and including radical reactions are plotted in Figure 4-5. Increasing the rate constant from 10 (● $k(H_2O_2)$ = 10) to 100 M^{-1} s^{-1} (◆ $k(H_2O_2$ = 100) increases the rate of oxidation of Tc(IV) by one order of magnitude, i.e. an increase of this rate constant by several orders of magnitude is needed to accommodate the experimental observations.

Another possibility that has been tested is to include very fast oxidation reactions with radical oxidants, such as $OH^•$ and $CO_3^{-•}$

$$TcO(OH)_2(aq) + OH^• \rightarrow products \qquad k = 10^8 \ M^{-1} \ s^{-1} \qquad\qquad (4.10)$$

$$TcO(OH)_2(aq) + CO_3^{-•} \rightarrow products \quad k = 10^8 \ M^{-1} \ s^{-1} \qquad\qquad (4.11)$$

These reactions would give the expected oxidation rate (■ $k(H_2O_2)$ = 10, $k(OH, CO_3^{-•})$ = 10^8 in Figure 4-5).

A definitive conclusion on the mechanism of Tc oxidation can not be reached because oxidation of the solid phase by heterogeneous electron transfer reactions and direct irradiation are processes that cannot be ruled out. Another possible reason could be that the H_2O_2 concentration locally was relatively high.

In addition there are uncertainties concerning the products of the oxidation of Tc(IV). In spite of a great number of studies on the aqueous electrochemistry of Tc, generally based on 1 to 3 electron reduction of TcO_4^-, the understanding of these processes are far from complete /Rard 1983/. Most electrochemical data do, however, provide evidence that TcO_4^{2-} and TcO_4^{3-} are the Tc(V) and Tc(VI) species, respectively, present in alkaline aqueous solutions. Pulse radiolysis studies on the one electron reduction of TcO_4^- also provide evidence for the formation of TcO_4^{2-} /Deutsch et al. 1978, Heller-Grossman et al. 1981, Libson et al. 1989/. According to /Pikaev et al. 1977/ TcO_4^{2-} protonates to $HTcO_4^-$ and H_2TcO_4 with pK_1 = 0.3 ± 0.8 and pK_2 = 8.7 ± 0.5, respectively. Both TcO_4^{2-} and TcO_4^{3-} are unstable in alkaline solution and disproportionate, ultimately forming TcO_4^- and Tc(IV).

One electron oxidation by *e.g.* OH$^\bullet$ and two-electron oxidation by H_2O_2

$$OH^\bullet + TcO(OH)_2 \rightarrow TcO_4^{3-} + 3\ H^+$$

$$H_2O_2 + TcO(OH)_2 \rightarrow TcO_4^{2-} + 2\ H^+ + H_2O$$
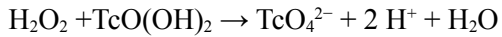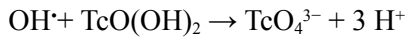
thus yield anionic species with sorption properties similar to those of TcO_4^-. These species are thus expected to be mobile in the pore water and not retarded by sorption on the solid phase.

The fate of these species is either to form TcO_4^- and Tc(IV) in disproportionation reactions or more probable undergo further oxidation in reactions with the radiolytically generated oxidants.

According to Cui and Eriksen /Cui and Eriksen 1996/ reduction of TcO_4^- by Fe(II) in the aqueous phase is, although thermodynamically possible, kinetically hindered. Reduction by heterogeneous electron transfer at the interface between groundwater and Fe(II)-bearing materials is expected to be an important retardation process for technetium /Vandergraaf et al. 1984, Haines et al. 1987, Cui and Eriksen 1996/. The distance travelled by technetium radiolytically oxidized to TcO_4^- will therefore be determined by the availability of Fe(II) bearing mineral surfaces along the diffusion and flow paths.
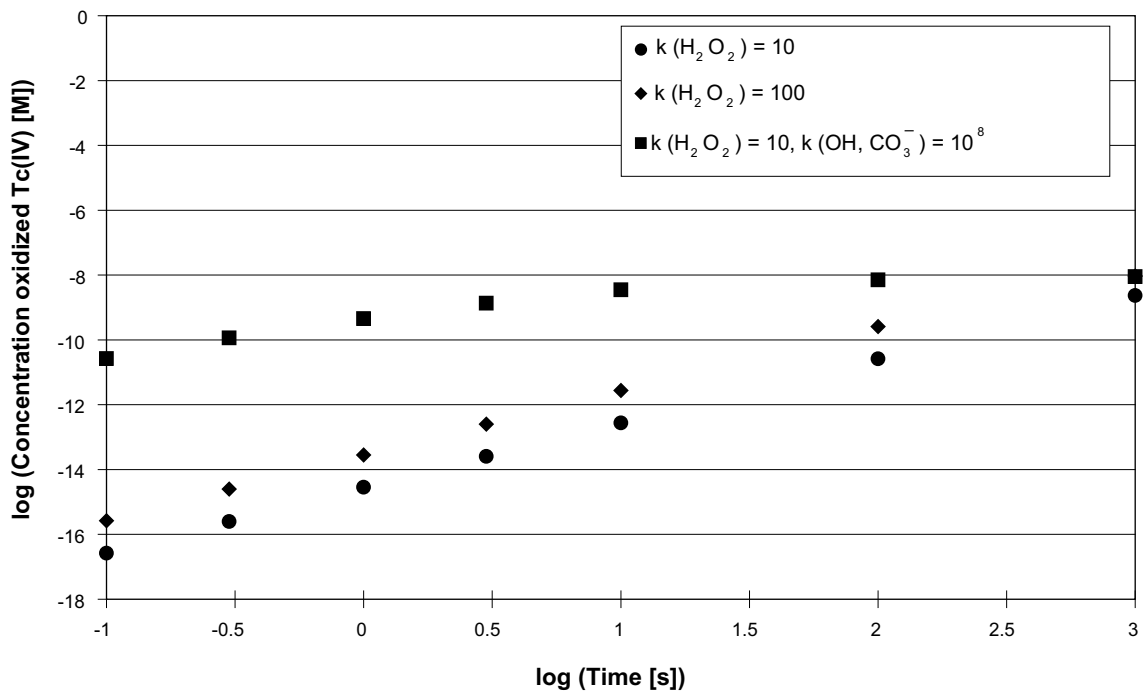
Figure 4-5. *Calculated concentration of oxidized Tc(IV) as a function of time. Initial concentrations of Tc(IV), HCO_3^- and Fe^{2+} were set to be 10^{-8} M, 0.36 mM and 1.7 µM, respectively. The rate constant for reaction 4.1c is varied between 10 $M^{-1}\ s^{-1}$ [● $k(H_2O_2)$ = 10] and 100 $M^{-1}\ s^{-1}$ [■ $k(H_2O_2$ = 100]. The effect of including very fast oxidation reactions with radical oxidants (reactions 4.10 and 4.11) are also shown [◆ $k(H_2O_2)$ = 10, $k(OH^\bullet,\ CO_3^{-\bullet})$ = 10^8].*

5   Conclusions

The experimental observations in the present CHEMLAB experiments as well as in an earlier CHEMLAB study in the same borehole on diffusive transport of TcO_4^- in compacted groundwater saturated bentonite /Jansson and Eriksen 2004/ are in accordance with data from laboratory experiments. The system studied is very complex comprising radiolysis, dissolution and diffusive processes, but the experimental data clearly indicate that the oxidation of Tc(IV) in the aqueous phase by O_2 is slow and that $OH^{\bullet}$ and $CO_3^{-\bullet}$ probably are involved in the oxidation process.

The possibility of Tc(IV) oxidation by heterogeneous electron transfer at the interface between solid $TcO_2 \cdot n H_2O$ and groundwater can not be excluded.

6   References

Carmström J, 2003. Kemiprovtagning och analys på Äspö. Sammanställning av kemi data januari–december 2002. SKB PIR-03-01, Svensk Kärnbränslehantering AB.

Carslaw H S, Jaeger JC, 1959. Conduction of Heat in Solids. 2nd ed. Clarendon Press, Oxford.

Carver M B, Hanley D V, Chaplin K R, 1979. MAKSIMA-CHEMIST. A Program for Mass Action Kinetics Simulation by Automatic Chemical Equation Manipulation and Integration Using Stiff Techniques, AECL – 6413.

Choppin G, Liljenzin J O, Rydberg J, 1996. Radiochemistry and Nuclear Chemistry, Butterworth-Heinemann, Oxford.

Cui D, Eriksen T E, 1996. Reduction of pertechnetate in solution by heterogeneous electron transfer from Fe(II)-containing geological material. Environ. Sci. Technol. 30(7), 2263–2269.

Deutsch E, Heineman W R, Hurst R, Sullivan J C, Mulac W A, Gordon S, 1978. Production, detection and characterization of transient hecavaletnt technetium in aqueous alkaline media by pulse radiolysis and very fast scan cyclic voltametry. J. Chem. Soc. Chem. Commun. 1034–40.

Ekeroth E, Jonsson M, 2003. Oxidation of UO_2 by radiolytic oxidants. J. Nucl. Mat. 322 242–248

Eriksen T E, Jacobsson A 1983. Radiation effects on the chemical environment in a radioactive waste repository. SKB TR-83-27, Svensk Kärnbränslehantering AB.

Eriksen T E, Christensen H, Bjergbakke E, 1987. Hydrogen production in α-irradiated bentonite Journal of Radioanalytical and Nuclear Chemistry 116, 13–25.

Eriksen T E, Ndalamba P, Christensen H, Bjergbakke E, 1988. Radiolysis of ground water: influence of carbonate and chloride on the hydrogen peroxide production, SKB TR-88-22, Svensk Kärnbränslehantering AB.

Eriksen T E, Cui D, 1991. On the interaction of granite with Tc(IV) and TC(VII) in aqueous solution. SKB TR-91-47, Svensk Kärnbränslehantering AB.

Eriksen T E, Ndalamba P, Bruno J, Caceci M, 1992. The solubility of $TcO_2 \cdot nH_2O$ in neutral to alkaline solutions under pCO_2. Radiochimica Acta 58–59 (Pt. 1) 67-70.

Haines R I, Owen R I, Vandergraaf T T, Nucl J, 1987. Canada 1:1, 32–37.

Heller-Grossman L, Abrashkin S, Schafferman A, Davis M A, Taube R A, 1981. [99m]Tc gengerators II, Physiochemical factors in the radiolytic reduction of pertechnetate, Int. J. Appl. Radiat. Isot. 32, 501–6.

Jansson M, Eriksen T E, 1998. CHEMLAB – in situ Diffusion Experiments using Radioactive Tracers. Radiochimica Acta 82, 153–156.

Jansson M, Eriksen T E, 2001. CHEMLAB A probe for in-situ radionuclide experiments. SKB TR-01-14, Svensk Kärnbränslehantering AB.

Jansson M, Eriksen T E, 2004. In situ anion diffusion experiments using radiotracers J. Cont. Hydr. Vol 68/3-4, pp 183–192

Libson K, Sullivan J C, Mulac W A, Gordon S, Deutsch E, 1989. Pulse radiolysis on pertechnetate and perrhenate in aqueous media. Decay of the technetium (VI) transient. Inorg. Chem. 28, 315-–9.

Marry V, Turq P, Cartailler T, Levesque D, 2002. Microscopic simulation of structure and dynamics of water and counterions in a monohydrated montmorillonite. J. Chem. Phys. 117 (7), 3454–3463.

Pikaev A K, Kryuchkov S V, Kuzina A F, Spitsyn V I, 1977. Pulsed radiolysis of neutral aqueous solutions of potassium pertechnetate, Dokl. Phys. Chem. 236, 992–5.

Pusch R, Karnland O, 1983. Aspects of the physical state of smectite absorbed water. SKB TR-83-37, Svensk Kärnbränslehantering AB.

Rard J A, 1983. Critical review of the chemistry and thermodynamics of technetium and some of its inorganic compounds and aqueous species. UCRL-53440, Lawrence Livermore National Laboratory.

Spinks J W T, Woods R J, 1990. An Introduction to Radiation Chemistry. 3rd ed. John Wiley & Sons, Inc. New York.

Vandergraaf T T, Ticknor K V, George I M, 1984. Geological Behaviour of Radioactive Waste, Barney, G.S., Navratil, J.D., Schultz, W.W. (eds) Am. Chem. Soc. Symp. Ser. 246, 24.